

## Role of Extracellular RNA and TLR3-Trif Signaling in Myocardial Ischemia–Reperfusion Injury

Chan Chen, MD, PhD;\* Yan Feng, MD, PhD;\* Lin Zou, MD, PhD;\* Larry Wang, MD, PhD; Howard H. Chen, PhD; Jia-Yan Cai, BS; Jun-Mei Xu, MD; David E. Sosnovik, MD; Wei Chao, MD, PhD

**Background**—Toll-like receptor 3 (TLR3) was originally identified as the receptor for viral RNA and represents a major host antiviral defense mechanism. TLR3 may also recognize extracellular RNA (exRNA) released from injured tissues under certain stress conditions. However, a role for exRNA and TLR3 in the pathogenesis of myocardial ischemic injury has not been tested. This study examined the role of exRNA and TLR3 signaling in myocardial infarction (MI), apoptosis, inflammation, and cardiac dysfunction during ischemia-reperfusion (I/R) injury.

**Methods and Results**—Wild-type (WT), TLR3<sup>-/-</sup>, Trif<sup>-/-</sup>, and interferon (IFN)  $\alpha/\beta$  receptor-1 deficient (IFNAR1<sup>-/-</sup>) mice were subjected to 45 minutes of coronary artery occlusion and 24 hours of reperfusion. Compared with WT, TLR3<sup>-/-</sup> or Trif<sup>-/-</sup> mice had smaller MI and better preserved cardiac function. Surprisingly, unlike TLR(2/4)-MyD88 signaling, lack of TLR3-Trif signaling had no impact on myocardial cytokines or neutrophil recruitment after I/R, but myocardial apoptosis was significantly attenuated in Trif<sup>-/-</sup> mice. Deletion of the downstream IFNAR1 had no effect on infarct size. Importantly, hypoxia and I/R led to release of RNA including microRNA from injured cardiomyocytes and ischemic heart, respectively. Necrotic cardiomyocytes induced a robust and dose-dependent cytokine response in cultured cardiomyocytes, which was markedly reduced by RNase but not DNase, and partially blocked in TLR3-deficient cardiomyocytes. In vivo, RNase administration reduced serum RNA level, attenuated myocardial cytokine production, leukocytes infiltration and apoptosis, and conferred cardiac protection against I/R injury.

**Conclusion**—TLR3-Trif signaling represents an injurious pathway during I/R. Extracellular RNA released during I/R may contribute to myocardial inflammation and infarction. (*J Am Heart Assoc.* 2014;3:e000683 doi: 10.1161/JAHA.113.000683)

**Key Words:** apoptosis • inflammation • ischemia • myocardial infarction • reperfusion • RNA • TLR

Heart diseases including ischemic myocardial infarction (MI) continue to be the leading cause of mortality in the US.<sup>1</sup> While reperfusion therapy such as percutaneous coronary intervention remains the most effective strategy to limit infarct size and preserve cardiac function, reperfusion itself

can cause injury to myocardium.<sup>2</sup> In response to ischemia-reperfusion (I/R), myocardial tissue exhibits marked innate immune responses as characterized by cytokine production and neutrophil infiltration<sup>2</sup> and cardiomyocyte apoptosis,<sup>3</sup> two major contributors to ischemic myocardial injury and left ventricular (LV) dysfunction.

Toll-like receptors (TLRs) are a critical component of the innate immune system and responsible for the host defense against foreign pathogens via pathogen-associated molecular pattern (PAMP) recognition.<sup>4</sup> Recent studies indicate that certain TLRs can also function as the sensors for endogenously produced ligands with danger-associated molecular pattern (DAMP). DAMP ligands are often produced upon tissue stresses such as ischemia, hypoxia, or trauma.<sup>5,6</sup> Examples of DAMP ligands include heat-shock proteins,<sup>7</sup> high mobility group box 1,<sup>8</sup> and RNA,<sup>9,10</sup> among others. All TLRs, with the exception of TLR3, signal through myeloid differentiation factor 88 (MyD88)-dependent pathways, whereas TLR3 exclusively and TLR4 partially signal via TIR domain-containing adaptor inducing IFN $\beta$ -mediated transcription factor (Trif). TLR3 was originally identified as the receptor for double-stranded RNA of viral origin.<sup>11</sup> Stimulation of TLR3-Trif

From the Department of Anesthesia, Critical Care and Pain Medicine (C.C., Y.F., L.Z., J.-Y.C., W.C.) and Martinos Center for Biomedical Imaging, Department of Radiology (H.H.C., D.E.S.), Massachusetts General Hospital, Harvard Medical School, Boston, MA; Department of Anesthesiology, the Second Xiangya Hospital, Central South University, Changsha, China (C.C., J.-M.X.); Department of Pathology and Laboratory Medicine, Children's Hospital of Los Angeles, Los Angeles, CA (L.W.).

Accompanying Figures S1 through S3 and Table S1 are available at <http://jaha.ahajournals.org/content/3/1/e000683/suppl/DC1>

\* Drs Chen, Feng, and Zou contributed equally to the study.

**Correspondence to:** Wei Chao, MD, PhD, Massachusetts General Hospital, Room 4.212, 149 13th Street, Charlestown, MA 02129. E-mail: [wchao@mgh.harvard.edu](mailto:wchao@mgh.harvard.edu)

Received November 21, 2013; accepted December 6, 2013.

© 2014 The Authors. Published on behalf of the American Heart Association, Inc., by Wiley Blackwell. This is an open access article under the terms of the Creative Commons Attribution-NonCommercial License, which permits use, distribution and reproduction in any medium, provided the original work is properly cited and is not used for commercial purposes.

signaling activates the transcriptional factors, NF- $\kappa$ B and interferon regulator factor 3/7 (IRF3/7), and subsequently results in the production of various cytokines such as type I IFN, which represents the major host antiviral mechanism.<sup>12</sup> Recent studies have suggested that TLR3 signaling may also recognize endogenous RNA released from necrotic cells in vitro,<sup>10,13,14</sup> mediates RNA-induced apoptosis in pancreatic  $\beta$ -cells<sup>15</sup> and cytokine production in various types of cultured cells.<sup>10,14</sup> In the heart, TLR3-Trif signaling is well known for its critical role in the host innate immune response against virus-induced myocarditis. Deficiency in TLR3-Trif signaling leads to an increased viral load, attenuated cytokine production, and increased mortality after viral infection such as coxsackievirus and encephalomyocarditis virus.<sup>16–18</sup> However, the role of TLR3-Trif signaling in the pathogenesis of myocardial ischemia-reperfusion injury is unknown.

In addition to its traditional role as the bridge molecule between DNA and protein, recent evidence suggest that extracellular RNA (exRNA) including microRNA (miRNA) and other non-coding RNA are found in all human body fluid examined and may play diverse roles such as cellular differentiation, chromatin modification, nuclear factor trafficking, inflammation, tissue injury/repair.<sup>19–26</sup> ExRNA, released from necrotic cells, mediates inflammatory responses in a variety of cell cultures including macrophages, fibroblasts, keratinocytes, and epithelial cells,<sup>10,13,14,27</sup> and may play a role in certain pathological conditions such as blood coagulation following vascular injury<sup>28</sup> and radiation-induced skin damage.<sup>14</sup> Whether or not exRNA plays a role in myocardial I/R injury is unclear.

Here, we hypothesized that TLR3-Trif signaling represents an injurious pathway in the heart and contributes to MI during I/R. We carefully tested the impact of TLR3-Trif deletion on myocardial cytokine responses, leukocyte infiltration, apoptosis, MI, and LV dysfunction after I/R. We examined the role of type I IFN, the downstream effector of TLR3-Trif signaling, in I/R-induced myocardial injury. We tested the release of RNA including microRNA from injured cardiomyocytes in vitro and ischemic myocardial tissue in vivo. Finally, we determined the role of exRNA in necrotic cell-induced cytokine responses in cardiomyocyte cultures and in a mouse model of myocardial I/R injury.

## Methods

### Genetic Mouse Models

C57BL/6J wild-type (WT) and TLR3<sup>-/-</sup> mice were purchased from the Jackson Laboratory. Trif<sup>-/-</sup> mice were generated by Yamamoto et al.<sup>29</sup> IFNAR1<sup>-/-</sup> mice were kindly provided by Dr Nir Hacohen at Massachusetts General Hospital (MGH). All

genetically modified mice were in C57BL/6J background. All animal care and procedures were performed according to the protocols approved by the Subcommittee on Research Animal Care of MGH.

### Myocardial Ischemia and Reperfusion Protocol

The surgical procedures of myocardial ischemia/reperfusion (I/R) injury were performed as previously described.<sup>30</sup> Briefly, male mice were anesthetized by intraperitoneal injection of ketamine (120 mg/kg) and xylazine (4 mg/kg), intubated, and ventilated. Body temperature was maintained at 36.5 to 37.5°C. A left intercostal thoracotomy was performed, and the left anterior descending coronary artery (LAD) was visualized and ligated with 7-0 silk sutures under a surgical microscope. For I/R injury, 45 minutes after LAD ligation, the ligature was released, and reperfusion was visually confirmed. Sham-operated mice underwent the same procedure without LAD ligation. The operators were blinded to the study design and intervention.

### Assessment of Myocardial Ischemic Area and Infarct Size

At the end of reperfusion, LAD was re-ligated. Fluorescent microspheres were injected into the left ventricle while the ascending aorta was briefly clamped as previously described.<sup>30</sup> The heart was isolated and cut into 5 sections. The areas devoid of microspheres were determined to be area-at-risk (AAR). To measure MI size, each section was stained with 1% triphenyltetrazolium chloride (TTC). Infarct size was calculated as the ratios of infarcted area (MI/LV,%) over AAR (AAR/LV,%), ie, MI/AAR  $\times$  100%.<sup>30</sup> Again, the operators were blinded to the information of study design and intervention.

### Echocardiographic Assessment of LV Structure and Function

Transthoracic echocardiographic (TTE) images were obtained using a 13.0-MHz linear probe (Vivid 7; GE Medical System) and interpreted by an echocardiographer blinded to the experimental design. M-mode images were obtained from a parasternal short-axis view at the mid-ventricular level with a clear view of papillary muscle. LV end-diastolic internal diameter (LVIDd) and LV end-systolic internal diameter (LVIDs) were measured. Fractional shortening (FS) was defined as  $([LVIDd - LVIDs] / LVIDd) \times 100\%$ . End-diastolic volume (EDV) and end-systolic volume (ESV) were measured using area-length method in 2-dimensional parasternal long axis view. Ejection fraction (EF) was calculated by the formula  $([EDV - ESV] / EDV) \times 100\%$  as previously described.<sup>30,31</sup> The values of three consecutive cardiac cycles were averaged.

## Myocardial Leukocyte Infiltration

Mouse myocardial leukocytes were isolated and quantified by flow cytometry following the protocol previously described.<sup>32,33</sup> After removing larger cardiomyocytes through a filter, smaller noncardiomyocytes were labeled, at 4°C for 30 minutes, with anti-CD45-PE-Cy5 and anti-Gr-1 mAb for neutrophil (BD Biosciences), anti-CD3-eFluor450 for T-lymphocytes (eBioscience), or anti-F4/80-FITC for macrophages (eBioscience).

## Cytokine Protein Measurement

Luminex multiplex fluorescent bead-based immunoassays were used to concurrently detect multiple cytokine expression in myocardial tissues as previously described.<sup>32</sup> To measure MIP-2, ELISA kits were used (R&D).

## Quantification of Cardiac Tissue and Cell Cytokine mRNA

qRT-PCR was performed on an Eppendorf PCR system. Data were normalized by the level of 18s or by GAPDH in each individual sample. The primer sequences used for qRT-PCR are listed in Table S1.

## C5b-9 Immunohistochemical Staining

C5b-9 deposition was detected immunohistochemically, using frozen myocardial tissue fixed in Acetone from 8 hearts. Immunostaining was performed with Leica BOND-MAX™ (Leica Microsystems Inc). The sections were incubated with anti-C5b-9 polyclonal rabbit antibody (Abcam: ab55811) at a dilution of 1:250 in Bond Primary Antibody Diluent (No. AR9352; Vision BioSystems Inc). Staining for C5b-9 deposition was visualized using Bond Polymer Refine Detection (No. DS9800; Leica Microsystems Inc). The slides stained for C5b-9 deposition were counterstained with hematoxylin. Appropriate positive and negative controls using mouse kidney were stained along with those slides.

## Ex Vivo Annexin V Imaging of Myocardial Cell Death

Fluorescence reflectance imaging (FRI) of myocardial cell death was performed using a conjugate of annexin V and a near-infrared fluorochrome (Annexin-Vivo 750=AV-750, Perkin Elmer). Mice were injected via tail vein with AV-750 at the onset of reperfusion. Four hours later, mice were euthanized for AV-750 imaging as we previously described.<sup>34</sup> In brief, the hearts were sectioned and multispectral FRI for AV-750 and red fluorescent microspheres was performed using the

appropriate filters on a commercial imaging system (IVIS Spectrum, Perkin Elmer). This allowed the area of cell death (AV-750 uptake) to be normalized to the AAR (absence of red microspheres).

## Apoptosis Assays

The apoptosis assays including DNA fragmentation and caspase-3 activity were measured as described previously.<sup>34,35</sup>

## Cardiomyocyte Isolation and Cultures

Rat and mouse neonatal cardiomyocytes were isolated and cultured as previously described with modifications.<sup>34,36</sup>

## NF-κB Activation

NF-κB activation was measured using a p65 Transcription Factor Kit (Thermo Scientific). A 96-well plate coated with a DNA binding sequence specific for active form of NF-κB. In brief, 20 mg heart tissue samples were lysed in 100 μL of M-PER lysis buffer and 25 μL of supernatant of lysate were loaded into the plate. After incubation and washing, the plate was incubated with antibody to p65, and then developed for luminescence.

## Necrotic Cell Treatment

Necrotic raw macrophages (Mφ) or cardiomyocytes in serum-free DMEM medium containing 0.05% BSA in 12-well plates were generated by freeze and thaw (3 cycles of 10 minutes freeze at −80°C followed by 10 minutes thaw at 37°C). Necrotic cell suspensions were stored at −80°C for later use. To test the effect of necrotic cells, rat or mouse neonatal cardiomyocytes were cultured in 12-well plates (for cellular cytokine RNA) or 96-well plate (for medium MIP-2 ELISA). The necrotic Raw Mφ or cardiomyocytes were incubated with cultured cardiomyocytes at the specific ratios (see figure legends for details) at 37°C for 8 hours in the presence or absence of RNase (2.8 U/mL) or DNase (2.8 U/mL). Cellular cytokine mRNA or medium cytokine protein was analyzed with qRT-PCR or ELISA, respectively.

## In Vivo RNase Administration and Serum Preparation

Bovine pancreatic RNase A (Invitrogen) was filtered through 30 kDa cut-off filter and stored at 4°C. As illustrated in Figure 9A, normal saline (N.S.) or 3 doses of RNase A were administered as follows: 500 μg/100 μL, sc, 30 minutes prior to, 200 μg/200 μL, ip, right before, and 500 μg/

100  $\mu$ L, sc, 2 hours after coronary occlusion. In the experiments designed to test serum RNase activity (Figure 9B), no surgical procedure was performed. Mouse blood was collected at 1 hour, 4 hours, and 24 hours after the second dose of RNase injection. To test serum RNase activity, serum was filtered through a 30-kDa cut-off filter to remove most serum proteins from RNase (17 kDa).

### MicroRNA Quantification

Total RNA was isolated from culture medium or serum using Trizol LS. *Caenorhabditis elegans* (*C. elegans*) microRNA (miRNA)-39 was added as the miRNeasy Serum/Plasma Spike-in Control. Reverse transcription was performed according to the miScript II RT kit. MicroRNA was quantified using miScript SYBR Green PCR kit following the manufacturer protocol (Qiagen). Relative miRNA expression was calculated using the comparative Ct method ( $2^{-\Delta\Delta Ct}$ ).

### Statistical Analysis

Statistical analysis was performed using Graphpad Prism 5 software. Unless stated otherwise, all data were expressed as means $\pm$ SE. For comparisons between groups (eg, sham versus I/R or 2 I/R groups), 2-tailed, unpaired Student *t* test was used for analysis of MI sizes, in vivo annexin V imaging, leukocyte infiltrations, and miRNA levels. To assess cardiac function changes over time (between the baseline and 24 h post-I/R) within a given group (eg, WT or KO), paired *t* test was used. Two-way ANOVA with Bonferroni post hoc test was

used for the other experiments. The null hypothesis was rejected for  $P<0.05$ .

## Results

### Genetic Deletion of TLR3 Reduces Myocardial Infarction and Improves Function after I/R

Compared with wild-type (WT) mice, mice deficient of TLR3 (TLR3<sup>-/-</sup>) had significantly smaller MI (28% reduction) as measured by TTC staining (MI/AAR=31 $\pm$ 5% versus 43 $\pm$ 3%,  $P<0.05$ ) following 45 minutes of coronary artery occlusion and 24 hours of reperfusion (Figure 1). Transthoracic echocardiography (TTE) studies indicated that left ventricle (LV) contractile function was similar between WT and TLR3<sup>-/-</sup> mice at the baseline (Figure 1, Table 1). Twenty-four hours after I/R, FS and EF in WT mice were decreased by 52% and 39% from the baseline, respectively ( $P<0.001$ ). Consequently, LVIDd and LVIDs were increased by 15% and 87%, respectively ( $P<0.001$ ). In comparison, TLR3<sup>-/-</sup> mice had significantly improved LV contractile function as demonstrated by better FS (+41%) and EF (+24%), and smaller LVIDs (-21%) ( $P<0.01$ ) (Table 1).

### TLR3 Deficiency Has No Impact on Myocardial Inflammation after I/R

TLR3 is known to regulate cellular inflammation via NF- $\kappa$ B and IRF3/7-type I interferon (IFN)<sup>11</sup> and plays a critical role in viral myocardial inflammation.<sup>16,17</sup> We tested whether or not TLR3

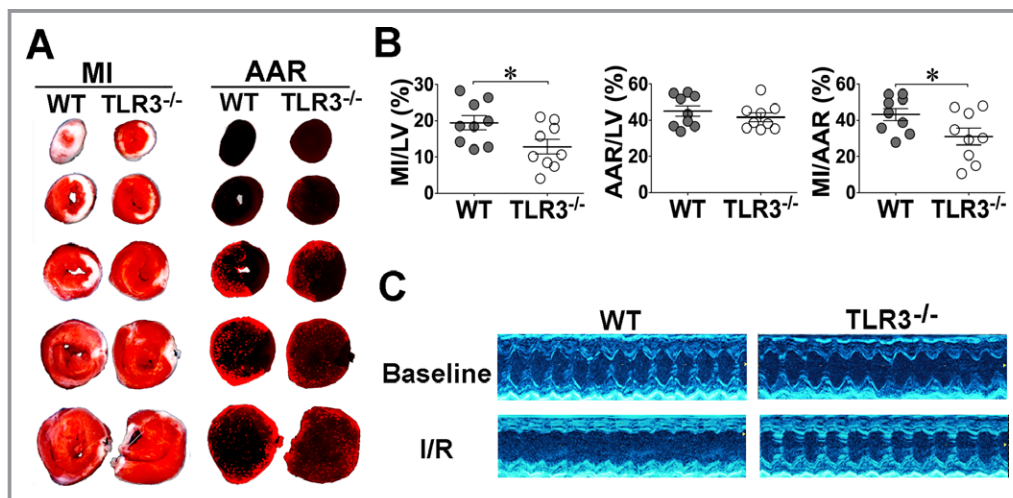


**Figure 1.** TLR3<sup>-/-</sup> mice have smaller MI and better-preserved cardiac function after I/R. A, Representative MI and AAR images of heart sections from WT and TLR3<sup>-/-</sup> mice after I/R (45 min/24 h). Infarcted myocardium is shown white, whereas AAR is the area devoid of red fluorescent light. B, Cumulative data of AAR and MI. C, Representative M-mode echocardiograms are from WT and TLR3<sup>-/-</sup> mice before (Baseline) and 24 hours after reperfusion (I/R). \* $P<0.05$ . AAR indicates area-at-risk; I/R, ischemia/reperfusion; LV, left ventricle; MI, myocardial infarction; TLR3, toll-like receptor 3; WT, wild type.



**Table 1.** Serial Echocardiographic Measurements Before and After I/R in WT and TLR3<sup>-/-</sup> Mice

	Baseline		24 Hours Post I/R		Changes Over Time (%)	
	WT	TLR3 <sup>-/-</sup>	WT	TLR3 <sup>-/-</sup>	WT	TLR3 <sup>-/-</sup>
HR, bpm	709±6	673±10	640±17 <sup>††</sup>	637±16	-10	-5
LVIDd, mm	3.3±0.1	3.3±0.1	3.8±0.1 <sup>††</sup>	3.5±0.1	15	6
LVIDs, mm	1.5±0.0	1.5±0.0	2.8±0.2 <sup>†††</sup>	2.2±0.2 <sup>**††</sup>	87	47
FS, %	56±1	54±1	27±2 <sup>†††</sup>	38±3 <sup>**†††</sup>	-52	-30
EF, %	75±1	77±2	46±3 <sup>†††</sup>	57±5 <sup>*†††</sup>	-39	-26
n	8	9	8	9		

Values are presented as mean±SE. Paired *t* tests were used for comparison within the groups (WT or TLR3<sup>-/-</sup>) and unpaired *t* tests for comparisons between the groups (WT vs TLR3<sup>-/-</sup>). EF indicates ejection fraction; FS, fractional shortening; HR, heart rate; I/R, ischemia/reperfusion; LVIDd, LV internal diameter at the end of diastole; LVIDs, LV internal diameter at the end of systole; TLR3, toll-like receptor 3; WT, wild type.

\**P*<0.05, \*\**P*<0.01 vs WT-I/R.

††*P*<0.01, †††*P*<0.001 vs TLR3<sup>-/-</sup>-baseline.

\*\**P*<0.01, †††*P*<0.001 vs WT-Baseline.

deficiency impacts on myocardial inflammation after I/R. To ensure the specific defect of TLR3 signaling in TLR3<sup>-/-</sup> mice, we treated isolated macrophages with TLR3 ligand. Poly I:C led to marked cytokine and type I/II IFN mRNA production in WT cells, but failed to do so in TLR3<sup>-/-</sup> cells (Figure S1). As shown in Figure 2A, WT and TLR3<sup>-/-</sup> mice had a basal level of cardiac cytokine protein expression and to our surprise, both had very similar, cytokine responses 24 hours after I/R, including IL-6, MCP-1, and CXCL1. Within the same time frame, WT and TLR3<sup>-/-</sup> mice had a significant increase only in IFN $\beta$  mRNA (Figure 2B). Moreover, while I/R induced a marked myocardial neutrophil influx in WT mice, there was no statistically significant difference between WT and TLR3<sup>-/-</sup> mice ( $9.0 \times 10^4$  versus  $12.4 \times 10^4$ ) (Figure 2C). Similarly, I/R induced marked C5b-9 deposition in the ischemic myocardium and there was no apparent difference between WT and TLR3<sup>-/-</sup> mice (Figure 3). These data suggest that the myocardial innate immune responses tested during I/R do not involve TLR3 signaling.

### Absence of Trif Signaling Reduces MI Sizes and Preserves LV Function

Trif is the adaptor molecule that is pivotal for both TLR3 and TLR4 signaling.<sup>29,37</sup> We tested if signaling via Trif was essential for I/R-induced MI. Figure 4A shows the representative photographs of MI and AAR of both WT and Trif<sup>-/-</sup> mice after I/R. The accumulated data in Figure 4B indicates that I/R resulted in 41±3% of MI (MI/AAR) in WT mice and 14±3% in Trif<sup>-/-</sup> mice, a 67% of reduction in MI size (*P*<0.001). TTE studies indicated that cardiac contractile function was similar between the 2 strains of mice at the baseline (Figure 4C, Table 2). Twenty-four hours after I/R, FS and EF in WT mice were decreased compared with the

baseline (*P*<0.001), and both LVIDd and LVIDs were significantly increased. Consistent with the MI data, Trif<sup>-/-</sup> mice had markedly improved LV contractile function as demonstrated by better FS (+44%) and EF (+39%) and smaller LVIDs (-25%) (*P*<0.01) when compared with WT mice following I/R (Table 2).

### Lack of Trif leads to Attenuated Myocardial Apoptosis in Ischemic Heart

Previous studies have shown that Trif signaling can effectively induce apoptosis when over expressed, suggesting a possible link between Trif signaling and apoptosis pathway.<sup>38</sup> To determine the underlying mechanism for the reduced myocardial injury in Trif<sup>-/-</sup> mice, we investigated the impact of Trif on myocardial apoptosis induced by I/R. WT and Trif<sup>-/-</sup> mice were subjected to 45 minutes of coronary occlusion and 4 hours of reperfusion. Myocardial apoptosis was assessed by ex vivo fluorescence reflectance imaging (FRI) of a near-infrared Annexin V conjugate (AV-750), DNA laddering, and caspase-3 activity. As illustrated in Figure 5, 4 hours of reperfusion resulted in significant MI and marked accumulation of fluorescent AV-750 in the myocardium (Figure 5A through 5C). Importantly, Trif<sup>-/-</sup> mice had smaller infarct sizes and reduced AV-750 accumulation compared with that of WT mice. Genomic DNA extracted from the ischemic myocardium of WT mice exhibited characteristic DNA laddering after I/R, whereas there was a marked decrease in DNA laddering in Trif<sup>-/-</sup> mice (Figure 5D). Finally, WT mice exhibited an increase in myocardial caspase-3 activity after I/R, whereas Trif<sup>-/-</sup> mice showed an attenuated level of caspase-3 activity (Figure 5E). Taken together, these data suggest that Trif signaling likely mediates an apoptosis pathway during cardiac I/R.

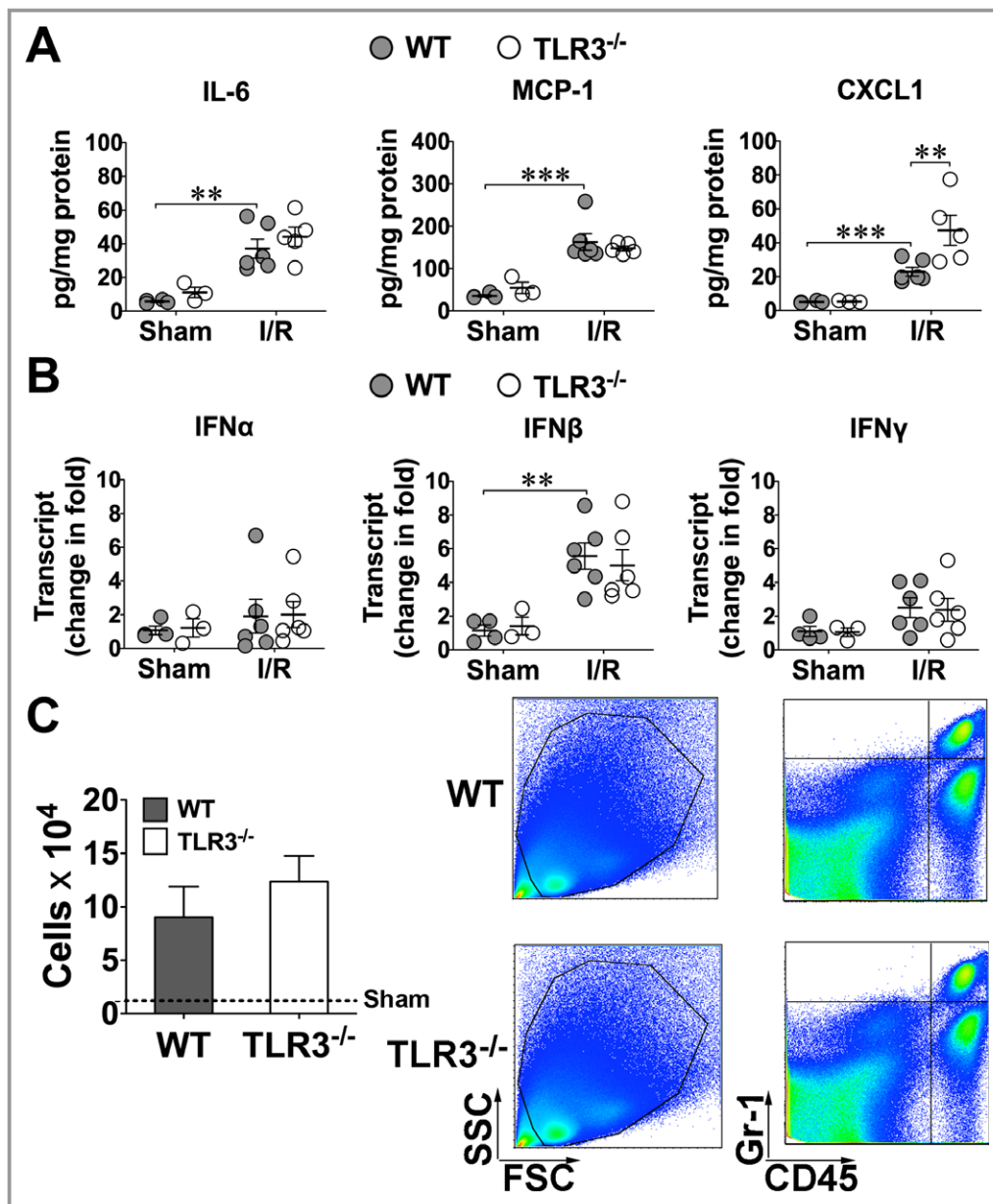


**Figure 2.** Loss of TLR3 has no impact on myocardial inflammation during I/R. WT and TLR3<sup>-/-</sup> mice were subjected to sham operation or coronary artery ligation for 45 minutes and then 24 hours of reperfusion. A, Cytokine proteins. At the end of reperfusion, myocardial cytokine protein production was measured by Luminex assays. B, Cytokine mRNA. C, Myocardial neutrophil infiltration after I/R. After enzymatic digestion, cardiomyocytes were removed and remaining cardiac cells were gated on CD45 and Gr-1 and analyzed with flow cytometry. Left, total CD45<sup>+</sup>/Gr-1<sup>+</sup> cells/heart in WT and TLR3<sup>-/-</sup> mice subjected to sham and I/R.  $n=3$  mice/group. Right, representative examples of FACS plots of myocardial cells from WT-I/R and TLR3<sup>-/-</sup>-I/R mice. FSC, forward scatter; SSC, side scatter. \*\* $P<0.01$ , \*\*\* $P<0.001$ . CXCL1 indicates chemokine (C-X-C motif) ligand 1; FACS, fluorescence-activated cell sorting; I/R, ischemia/reperfusion; IFN, interferon; IL, interleukin; MCP-1, monocyte chemoattractant protein-1; TLR3, toll-like receptor 3; WT, wild type.

### Trif Signaling Has No Effect on Myocardial Inflammation During I/R

We confirmed that Trif deficiency specifically blocked TLR3-mediated cytokine response as described in Figure S2. In vivo, 24 hours of reperfusion induced a significant increase in myocardial IL-6, MCP-1, CXCL1 expression (Figure 6A), whereas 4 hours of reperfusion induced a significant increase

in both type I/II IFN mRNA production (Figure 6B). To our surprise, absence of Trif had no effect on the level of myocardial cytokine expression (Figure 6A and 6B). Moreover, there was no difference between WT and Trif<sup>-/-</sup> in the total numbers of CD45<sup>+</sup> and Gr-1<sup>+</sup> neutrophils recruitment ( $14.5 \times 10^4$  versus  $13.3 \times 10^4$ ) after I/R. In contrast, MyD88 deficiency resulted in a marked reduction in neutrophil infiltration (Figure 6C). These data suggest that TLR3-Trif

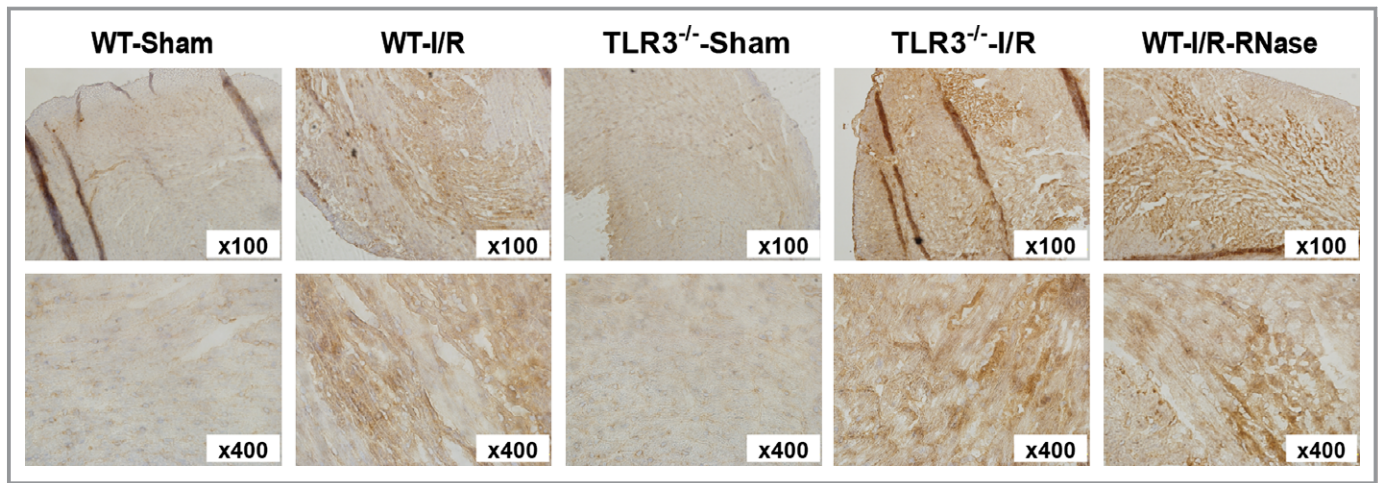


**Figure 3.** C5b-9 myocardial deposition following I/R. WT or TLR3<sup>-/-</sup> mice were subjected to either Sham or I/R. RNase was administered to WT mice according to a protocol described in the Methods. Twenty-four hours after LAD ligation, mice were euthanized, the heart sectioned and stained for C5b-9 as described in the Methods. I/R indicates ischemia/reperfusion; LAD, left anterior descending coronary artery; TLR3, toll-like receptor 3; WT, wild type.

signaling plays no major contributory role in myocardial cytokine response and neutrophil recruitment following I/R.

### Absence of Type I IFN Receptor Does Not Change MI Size Following I/R

One of the key downstream effectors of TLR3-Trif signaling is Type I IFN,<sup>39,40</sup> which is critical for mediating myocardial inflammation during the early phase of viral infection.<sup>18</sup> We wondered if Type I IFN would mediate myocardial injury after I/R. IFNAR, including the subunits IFNAR1 and IFNAR2, are the binding sites of type I IFNs.<sup>41</sup> Mice lacking IFNAR are

completely unresponsive to type I IFN.<sup>42</sup> We subjected IFNAR1<sup>-/-</sup> mice to the same I/R protocol as that of WT and Trif<sup>-/-</sup> mice and found no difference in MI sizes (Figure S3) or LV function (data not shown) between IFNAR1<sup>-/-</sup> and WT mice. These data suggest that type I IFN is not responsible for I/R-induced myocardial injury.

### RNA Is Released from Injured Macrophages and Cardiomyocytes

We stained intracellular RNA with SYTO-RNaselect Stain (SYTO), a cell-permeable and highly RNA-selective fluorescent

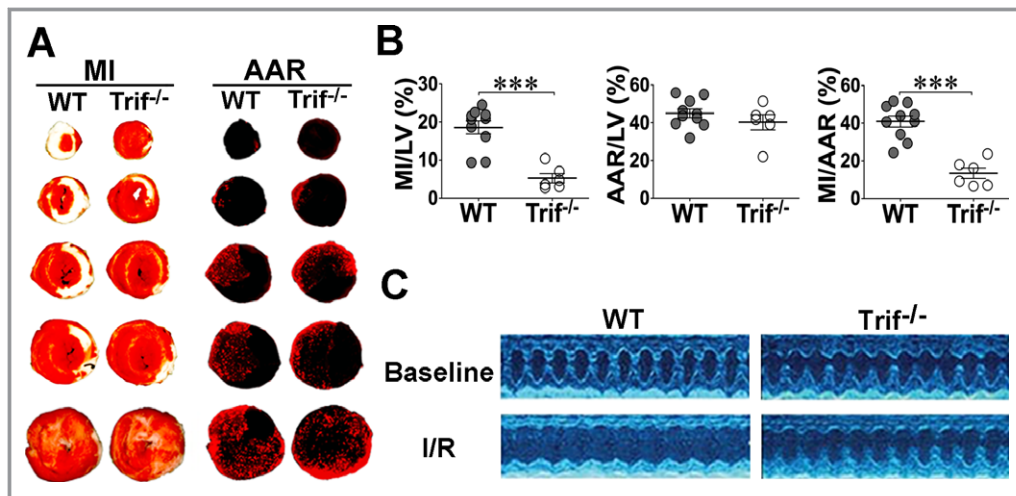


**Figure 4.** Trif<sup>-/-</sup> mice have reduced MI and better-preserved cardiac function after I/R. A, Representative MI and AAR images of heart sections from WT and TLR3<sup>-/-</sup> mice after I/R. Infarcted myocardium is shown white, whereas AAR is the area devoid of red fluorescent light. B, Cumulative data of MI and AAR. C, Representative M-mode echocardiograms of WT and Trif<sup>-/-</sup> mice before (baseline) and 24 hours after I/R. \*\*\**P*<0.001. AAR indicates area-at-risk; I/R, ischemia/reperfusion; LV, left ventricle; MI, myocardial infarction; TLR3, toll-like receptor 3; Trif, TIR domain-containing adaptor inducing IFN $\beta$ -mediated transcription factor; WT, wild type.

**Table 2.** Serial Echocardiographic Measurements Before and 24 Hours After I/R in WT and Trif<sup>-/-</sup> Mice

	Baseline		24 Hours Post I/R		Changes Over Time (%)	
	WT	Trif <sup>-/-</sup>	WT	Trif <sup>-/-</sup>	WT	Trif <sup>-/-</sup>
HR, bpm	699±6	700±19	697±17	654±21	0	-7
LVIDd, mm	3.2±0.1	3.2±0.0	3.6±0.1 <sup>‡</sup>	3.4±0.1	13	6
LVIDs, mm	1.4±0.0	1.5±0.1	2.4±0.2 <sup>‡‡</sup>	1.8±0.2 <sup>**</sup>	71	20
FS, %	57±1	55±2	32±4 <sup>‡‡‡</sup>	46±4 <sup>**†</sup>	-44	-16
EF, %	81±2	81±2	49±6 <sup>‡‡</sup>	68±7 <sup>*</sup>	-40	-16
n	6	5	6	5		

Values are presented as mean±SE. Paired *t* tests were used for comparison within the groups (WT or TLR3<sup>-/-</sup>) and unpaired *t* tests for comparisons between the groups (WT vs TLR3<sup>-/-</sup>). EF indicates ejection fraction; FS, fractional shortening; HR, heart rate; I/R, ischemia/reperfusion; LVIDd, LV internal diameter at the end of diastole; LVIDs, LV internal diameter at the end of systole; Trif, TIR domain-containing adaptor inducing IFNβ-mediated transcription factor; WT, wild type.

\**P*<0.05, \*\**P*<0.01 vs WT-I/R.

†*P*<0.05 vs Trif<sup>-/-</sup>-baseline.

‡*P*<0.05, ‡‡*P*<0.01, ‡‡‡*P*<0.001 vs WT-baseline.

dye.<sup>43</sup> SYTO-stained RNA was located primarily in the nucleus (Figure 7A). To detect exRNA, cells were treated without or with 2 injurious conditions including freeze and thaw or hypoxia/serum deprivation (Figure 7B). In untreated cells (None), RNA was located in cells and mainly in 3 sizes, 28S, 18S, and small molecular weights. However, in necrotic cell cultures, both macrophages (Mφ) and isolated rat cardiomyocytes (CM), exRNA was detected in the culture media as stained by SYTO (Figure 7B). RNase, but not DNase, completely digested the SYTO-stained exRNA in vitro (Figure 7B). Moreover, qRT-PCR demonstrated that injured cardiomyocytes released miRNA into the media including miR-208a (2285-fold), miR499 (752-fold), miR-1 (147-fold), and miR-133 (45-fold) after hypoxia/serum deprivation (Figure 7C).

### Necrotic Mφ and Cardiomyocytes Induce Cytokine Response in Cardiomyocytes—Role of RNA and TLR3

When treated with necrotic Mφ, rat cardiomyocytes produced multiple cytokine mRNA including IL-1β (12.1-fold), MIP-2 (16.4-fold), IL-6 (11.8-fold), CXCL1 (5.5-fold), and MCP-1 (14.7-fold) (Figure 8A). When necrotic cells were pretreated with RNase, cytokine mRNA responses were either abolished (IL-1β) or significantly inhibited (MIP-2, IL-6, CXCL1). In contrast, the same concentration of DNase had no effect on the cytokine production. We also tested MIP-2 protein production in cardiomyocytes in response to necrotic Mφ and cardiomyocytes (Figure 8B). Rat cardiomyocyte cultures were treated with 2 concentrations of necrotic Mφ or cardiomyocytes in the presence or absence of RNase or DNase. Both necrotic Mφ and rat cardiomyocytes induced a dose-dependent increase in MIP-2 protein production. Again, RNase but not DNase attenuated the cytokine response.

Necrotic cardiomyocytes also induced an equally robust MIP-2 response in cardiac fibroblasts (data not shown). Moreover, to determine if necrotic cell-induced cytokine response was mediated by TLR3, we tested the effect of necrotic cardiomyocytes in WT and TLR3<sup>-/-</sup> mouse cardiomyocytes. Similar to rat cardiomyocytes, WT mouse cardiomyocytes produced MIP-2 in response to necrotic rat cardiomyocytes in a dose-dependent manner. TLR3<sup>-/-</sup> cardiomyocytes also responded to the necrotic cells but at much attenuated levels as compared with WT cardiomyocytes (Figure 8C). Of note, these cultured TLR3<sup>-/-</sup> cardiomyocytes responded normally to LPS, a TLR4 ligand, as did WT cells, but failed to respond to poly I:C. Taken together, these data clearly demonstrate that cellular RNA is released from cardiomyocytes upon injury and that necrotic cells, both macrophages and cardiomyocytes, are capable of inducing robust cytokine responses in cardiomyocytes through RNA- and TLR3-dependent mechanisms.

### Role of exRNA in Myocardial Inflammation and Injury Following I/R

Similar to cultured cardiomyocytes subjected to hypoxia/serum deprivation in vitro (Figure 7B and 7C), transient myocardial ischemia in vivo (45 minutes of ischemia and 3 hours of reperfusion) induced a marked increase in circulating plasma RNA including miR-208a (4.0-fold), miR-499 (8.6-fold), miR-1 (6.4-fold), and miR-133 (4.9-fold), presumably released from the ischemic myocardium (Figure 7D). To explore the role of exRNA in ischemic myocardial injury, we administered RNase to animals as described previously.<sup>28</sup> The in vivo RNase administration protocol (Figure 9A) led to an increased serum RNase activity for up to at least 4 hours as evidenced by an enhanced RNA degradation in vitro (Figure 9B) and significant reduction in



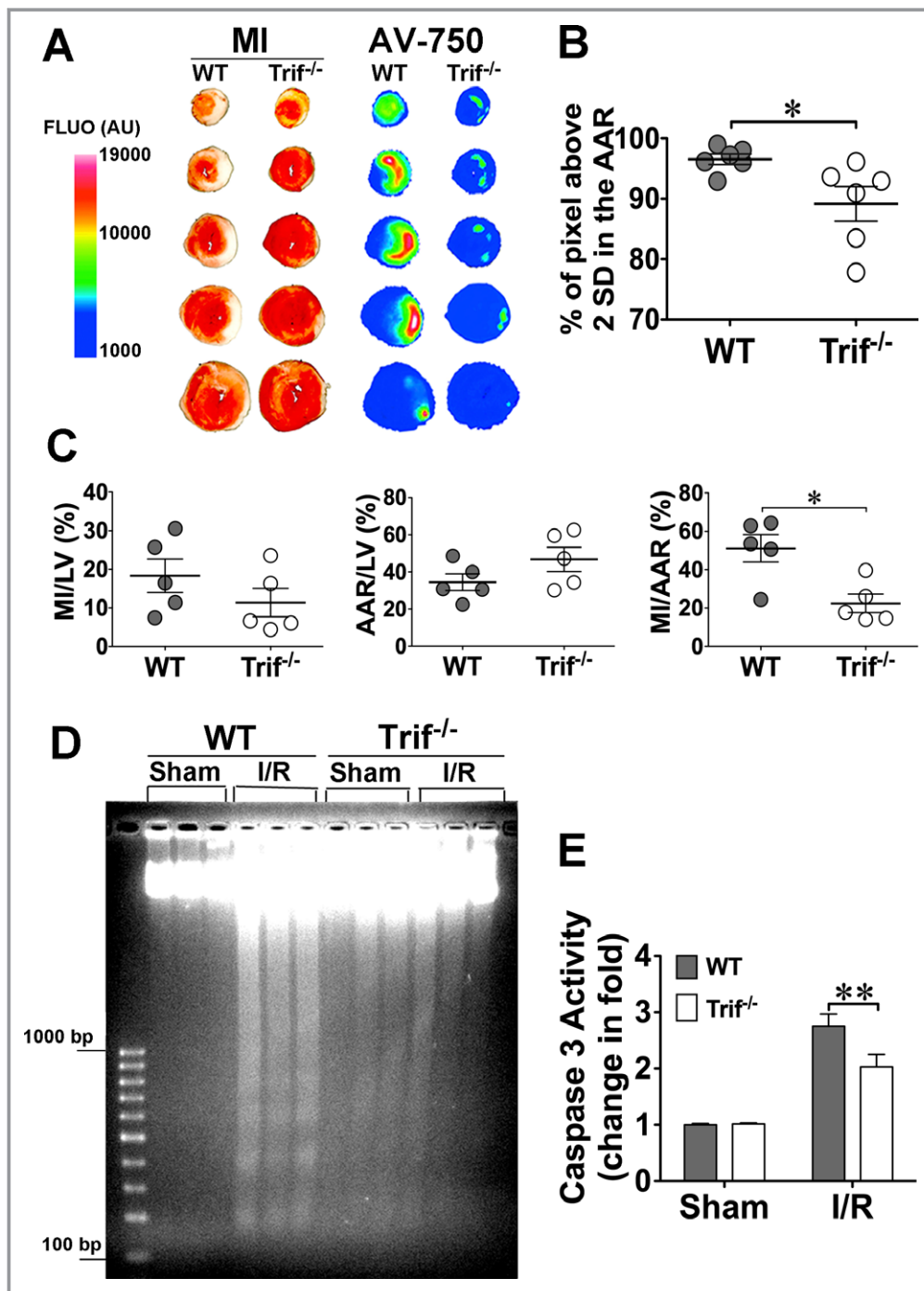


**Figure 5.** Trif<sup>-/-</sup> mice have attenuated myocardial apoptosis and decreased caspase-3 activity. A, Representative images of TTC stained myocardium section (*left*) and the corresponding fluorescence reflectance images of fluorescent annexin V construct, AV-750, injected at the onset of reperfusion (*right*), were acquired at 4 hours of reperfusion from WT and Trif<sup>-/-</sup> mice. B, The area of annexin positivity, expressed as the percentage of pixels in the AAR with an AV-750 signal >2 SD above background, is significantly reduced in the Trif<sup>-/-</sup> mice. C, Cumulative data of AAR and MI. D, Myocardial DNA fragmentation. Genomic DNA was isolated 4 hours after reperfusion and subjected to agarose gel electrophoresis. E, Myocardial caspase-3 activity was assayed after I/R (45 min/4 h). Sham, n=8 mice/group; I/R, n=10 mice/group. \*P<0.05, \*\*P<0.01. AAR indicates area-at-risk; AV-750, Annexin-Vivo 750; I/R, ischemia/reperfusion; LV, left ventricle; MI, myocardial infarction; Trif, TIR domain-containing adaptor inducing IFN $\beta$ -mediated transcription factor; TTC, triphenyltetrazolium chloride; WT, wild type.

the circulating endogenous miRNA (miR-1 and miR-133) in both Sham and I/R mice (Figure 9C). Moreover, compared with mice administered with normal saline, mice treated with

3 doses of RNase as detailed in Figure 9A had significantly reduced myocardial cytokine responses including CXCL1, IL-1 $\beta$ , IL-6, MIP-2, and TNF $\alpha$  (Figure 10A), attenuated

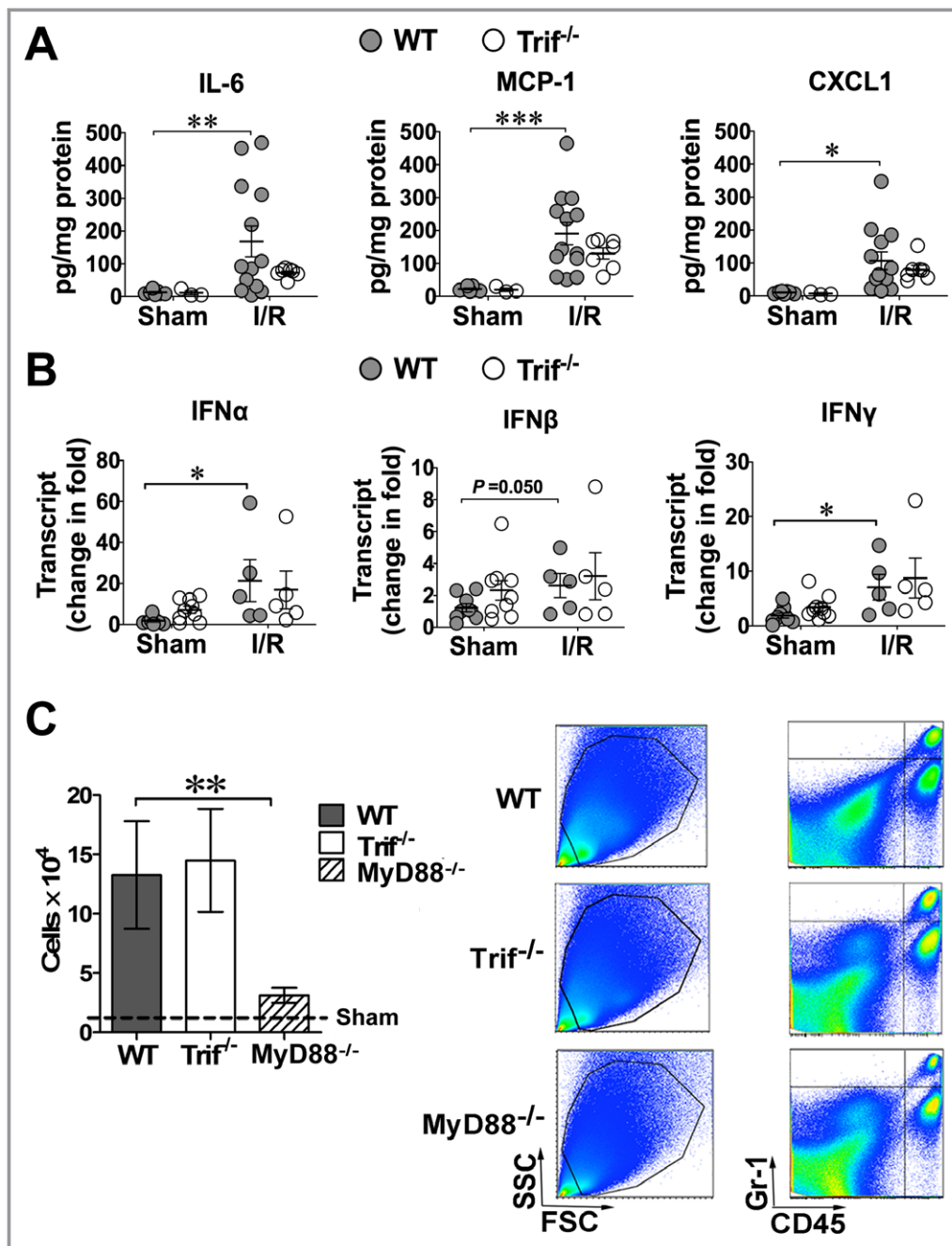


**Figure 6.** Lack of Trif has no impact on myocardial inflammation after I/R. Mice were subjected to I/R (45 min/4 h or 24 h). A, Myocardial cytokine protein expression. Twenty-four hours after reperfusion, cytokine proteins were measured using Luminex. B, Myocardial cytokine mRNA. Four hours after reperfusion, IFN mRNAs were assayed using qRT-PCR. C, Myocardial neutrophil infiltration after I/R. Left, total CD45<sup>+</sup>/Gr-1<sup>+</sup> cells in the hearts of WT, Trif<sup>-/-</sup>, or MyD88<sup>-/-</sup> mice that were subjected to sham or I/R. n=3 mice/group. Right, representative examples of FACS plots of myocardial cells from mice subjected to I/R. FSC, forward scatter; SSC, side scatter. \**P*<0.05, \*\**P*<0.01, \*\*\**P*<0.001. CXCL1, chemokine (C-X-C motif) ligand 1; I/R, ischemia/reperfusion; IFN, interferon; IL, interleukin; MCP-1, monocyte chemoattractant protein-1; MyD88, myeloid differentiation factor 88; qRT-PCR, quantitative real time polymerase chain reaction; Trif, TIR domain-containing adaptor inducing IFN $\beta$ -mediated transcription factor; WT, wild type.

myocardial CD45<sup>+</sup>/Gr-1<sup>+</sup> neutrophil and CD3<sup>+</sup> T lymphocyte infiltration (Figure 10B), a tendency of reduced NF- $\kappa$ B activity (Figure 10C), and decreased myocardial caspase-3 activity (Figure 10D) after I/R. However, while I/R induced marked C5b-9 deposition in the ischemic myocardium, RNase treat-

ment had no apparent effect on the complement deposition (Figure 3). Finally, RNase-treated mice had modest but significantly smaller MI compared with the saline-treated control mice (MI/AAR: 23 $\pm$ 3% vs 33 $\pm$ 2%, 30% reduction, *P*<0.01) at 24 hours after I/R (Figures 10E and 10F). Taken together,

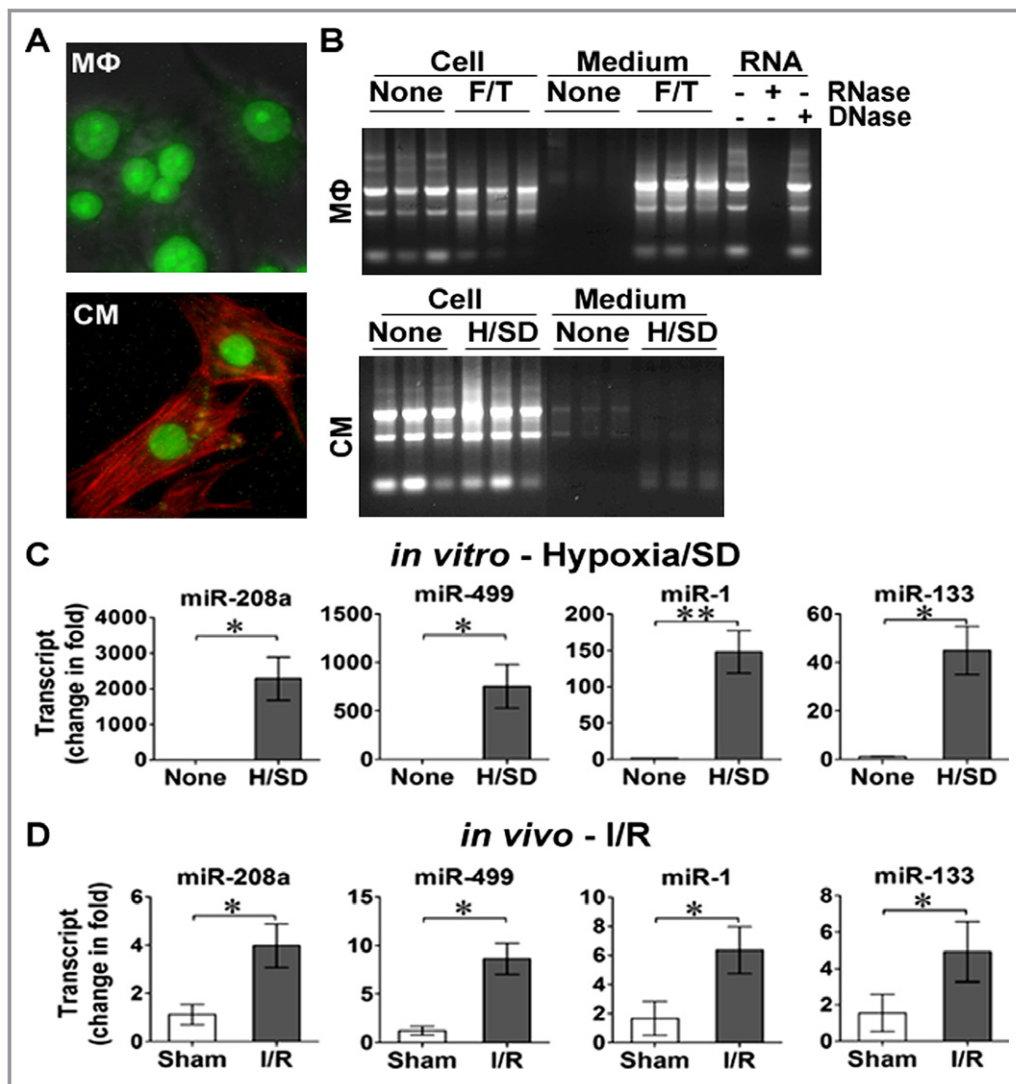


**Figure 7.** RNAs are released from injured cells in vitro and ischemic myocardium in vivo. A, Representative pictures of SYTO-stained intracellular RNA in macrophages (Mφ) and in rat cardiomyocytes (CM). SYTO RNA-select green fluorescent dye was used to stain intracellular RNA. CM were also co-stained for troponin T shown in red. B, SYTO fluorescent imaging of RNA gel electrophoresis. Mφ and CM were subjected various injurious conditions as follows: Freeze/thaw (F/T), 3 cycles  $\times$  10 minutes at  $-80^{\circ}\text{C}$  followed by 10 minutes  $\times$  3 at  $37^{\circ}\text{C}$ ; H/SD, hypoxia in serum/glucose-free medium for 24 hours. Cells and media were harvested separately and extracted for RNA with Trizol and Trizol LS, respectively. Purified RNA was stained with SYTO fluorescence dye followed by gel electrophoresis. In separate experiments, the same amount of purified RNA was incubated without or with RNase or DNase before SYTO staining and gel electrophoresis. C, miRNA is released from hypoxic rat CM in vitro. Cultured CM were subjected to hypoxia/SD for 24 h, whereas control CM (None) were briefly treated with serum-free RPMI-1640 medium for 5 minutes.  $n=3/\text{group}$ . D, Circulating miRNA after sham or myocardial I/R (45 min/3 h)  $n=3$  mice/group. To measure miRNA, culture media or sera were extracted for total RNA using Trizol LS. miRNA were measured by qRT-PCR using miScript II RT and miScript SYBR Green PCR kits. Cel-miR-39 was used as the spike-in control.  $*P<0.05$ ,  $**P<0.01$ . I/R indicates ischemia/reperfusion; miRNA, microRNA; qRT-PCR, quantitative real time polymerase chain reaction.

these data suggest that RNA is released from ischemic myocardium following I/R and exRNA may play a role in mediating myocardial inflammation, apoptosis, and infarction.

## Discussion

We have made 4 major observations in this study. First, we show that genetic deletion of TLR3 or Trif confers a significant

protection against ischemic myocardial injury with reduced infarct size and improved LV function. Second, we demonstrate that signaling via Trif mediates myocardial apoptosis during I/R as evidenced by reduced cardiac AV-750 fluorescent signals in ischemic myocardium, reduced DNA laddering, and attenuated caspase-3 activation in  $\text{Trif}^{-/-}$  animals. Unlike its critical role in myocardial innate immune response against viral myocarditis and distinctly different from TLR2/

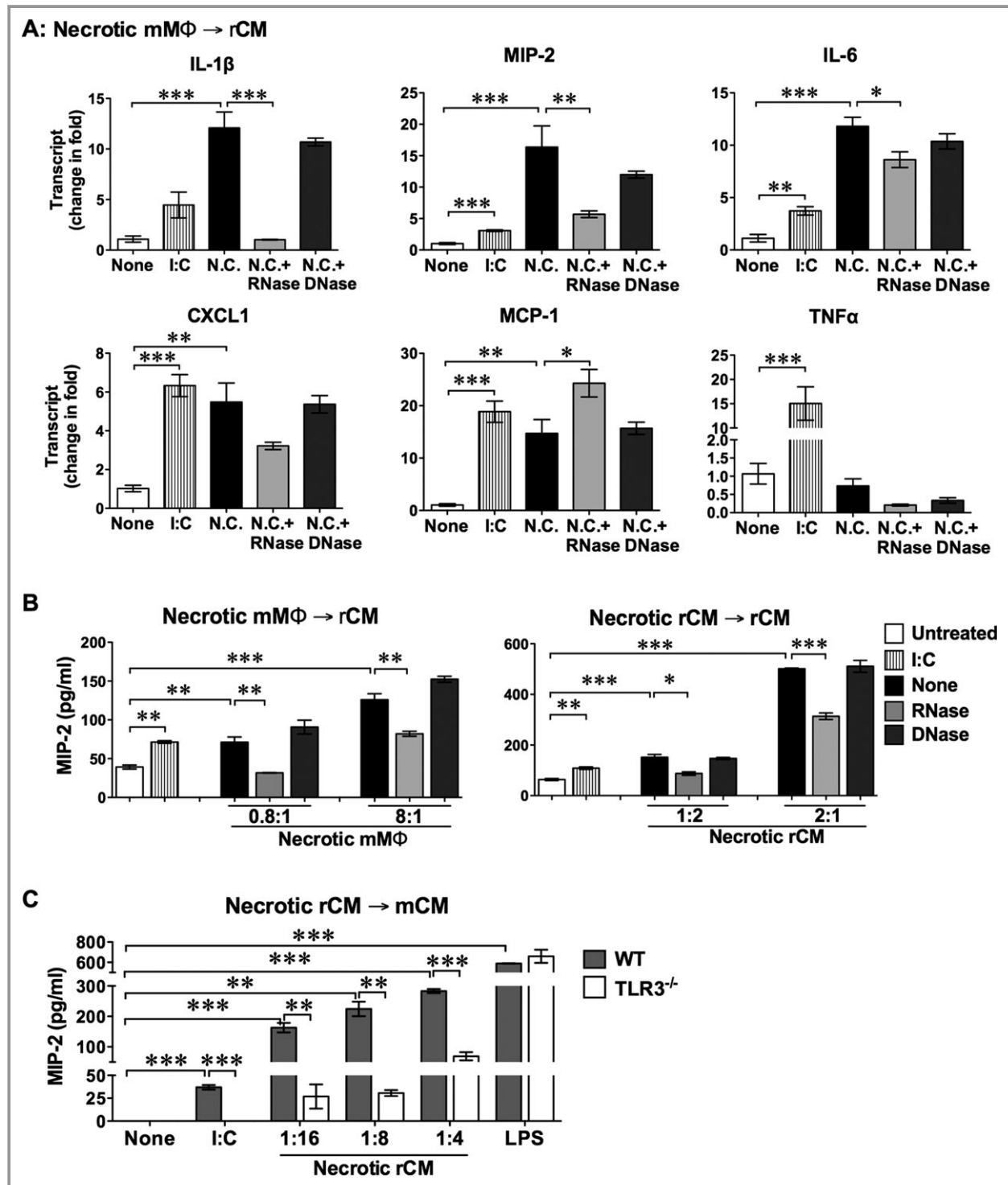


**Figure 8.** Necrotic Mφ and cardiomyocytes induce robust cytokine production. A, Necrotic mouse macrophages (mMφ) induce cytokine mRNA production in rat cardiomyocytes (rCM). Cultured rCM ( $0.8 \times 10^6$  cells/well in 12-well plate) were incubated with necrotic (N.C.) mMφ (N.C./culture cells ratio=4/1) in the absence or presence of 2.8 U/mL of RNase or DNase as indicated for 8 hours. Poly:I:C (I:C) is a TLR3 ligand. B, Necrotic cells induce MIP-2 protein production in rCM. Necrotic mMφ or rCM preparations were added to rCM cultures ( $0.8 \times 10^5$  cells/well in 96-well plate) in the presence or absence of RNase or DNase for 8 hours. Medium MIP-2 was assayed. The ratios represent N.C./culture cells. C, MIP-2 production in culture media of WT and TLR3<sup>-/-</sup> mouse CM (mCM). Necrotic CM were incubated with WT or TLR3<sup>-/-</sup> mCM ( $1.1 \times 10^5$  cells/well in 96-well plate) for 8 hours. Medium MIP-2 was assayed. I:C, poly I:C, 20 μg/mL; LPS, lipopolysaccharide, 10 ng/mL. Each data point in A through C represents mean±SE of triplicate measurements and each experiment was repeated 3 times. \* $P < 0.05$ , \*\* $P < 0.01$ , \*\*\* $P < 0.001$ . CXCL1 indicates chemokine (C-X-C motif) ligand 1; I/R, ischemia/reperfusion; IFN, interferon; IL, interleukin; MCP-1, monocyte chemoattractant protein-1; MIP-2, macrophage inflammatory protein-2; TLR3, toll-like receptor 3; WT, wild type.



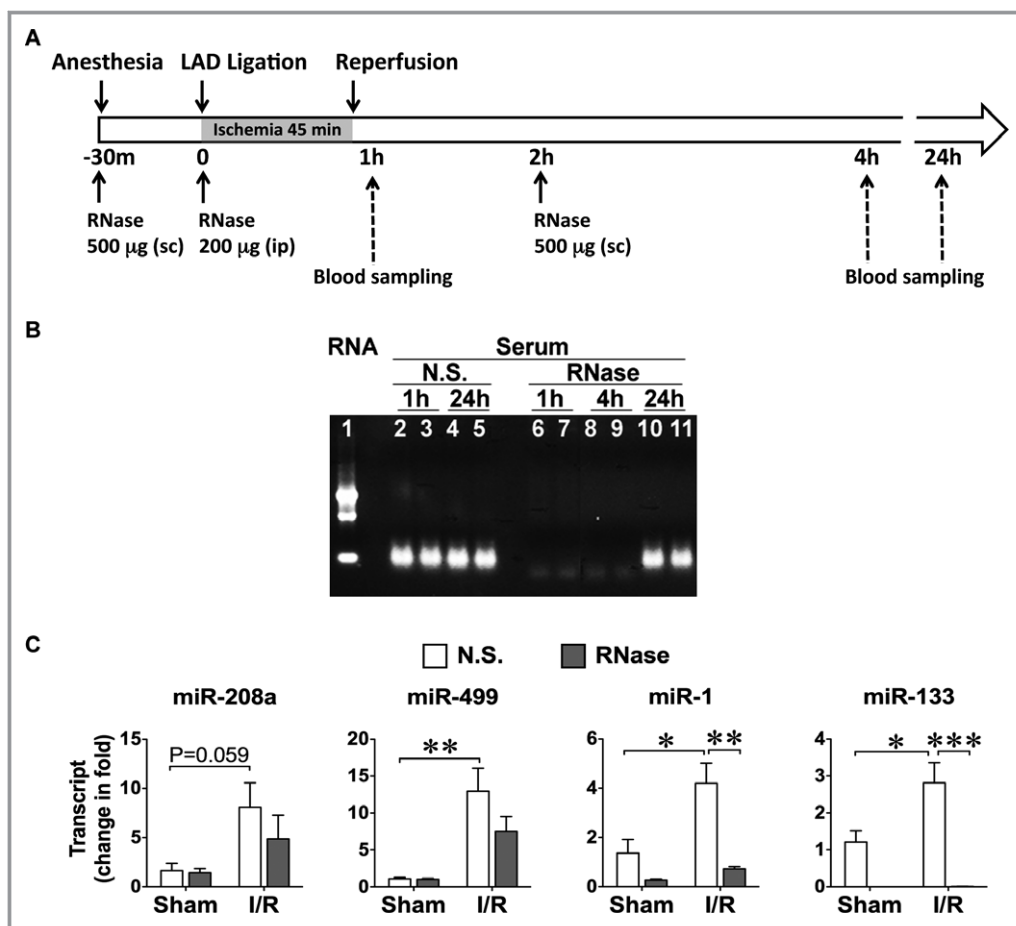


**Figure 9.** In vivo administration of RNase A increased serum RNase activity. A, Experimental protocol of RNase injection, LAD ligation, and blood sampling. Three doses of RNase A (or normal saline, N.S., not shown) were administered as follows: 500 µg/100 µL, sc, 30 minutes prior to, 200 µg/200 µL, ip, right before, and 500 µg/100 µL, sc, 2 hours after LAD ligation. B, RNA digestion by serum RNase. No surgical procedure was performed in this set of experiments. Mouse blood was collected at 1 hour, 4 hours, and 24 hours after the second dose of N.S. or RNase as indicated above and serum was prepared. Serum was filtered through a 30-kDa cut-off filter to remove most of serum proteins. Filtered serum was incubated with 1.5 µg of purified Raw Mφ RNA at 37°C for 2 hours followed by SYTO staining and RNA gel electrophoresis. Lane 1: Untreated RNA, Lane 2-5: RNA treated with serum from saline-treated mice; Lane 6-11: RNA treated with serum from RNase-treated mice. C, Effect of RNase A on serum endogenous miRNA. Mice treated with N.S. or RNase as noted above were subjected to sham or I/R. Three hours after reperfusion, serum was collected and analyzed for miRNA. Sham, n=3; I/R, n=7. I/R indicates ischemia/reperfusion; LAD, left anterior descending coronary artery; miRNA, microRNA.

4-MyD88 signaling,<sup>30,32,44,45</sup> TLR3-Trif signaling exhibits minimal impact on myocardial cytokine response including its downstream effector type I IFN and on myocardial neutrophil infiltration during I/R. Third, we show that cellular RNA is released from injured cardiomyocytes in vitro and from ischemic myocardium in vivo and that necrotic cells induce robust cytokine responses in cardiomyocytes, which is markedly reduced by RNase and significantly blocked in TLR3<sup>-/-</sup> cardiomyocytes. Finally, in vivo RNase administration reduces serum RNA level, attenuates myocardial cytokine production and leukocytes infiltration, and confers significant cardiac protection against I/R injury.

Previous studies show that genetic deletion or pharmacological inhibition of TLR2/4 or their adaptor molecular MyD88

leads to reduced myocardial cytokine production, attenuated neutrophil recruitment, decreased C3 deposition, and reduced MI.<sup>30,32,34,44-46</sup> TLR2/4-MyD88 signaling may contribute to I/R-induced myocardial injury by mediating a pro-inflammatory response in ischemic heart.<sup>6</sup> In addition to controlling the myocardial environment such as local cytokine production, TLR2/4-MyD88 signaling may also modulate the functions of circulating neutrophils.<sup>30,32,44,47</sup> In an in vivo model of neutrophil migration and a chimeric model of MyD88 deletion, we have shown that MyD88 signaling is essential for maintaining neutrophil migratory function and the chemokine receptor CXCR2 expression and that MyD88 signaling in circulating neutrophils plays a critical role in I/R-induced myocardial injury.<sup>32</sup> Similarly, the current study demonstrates

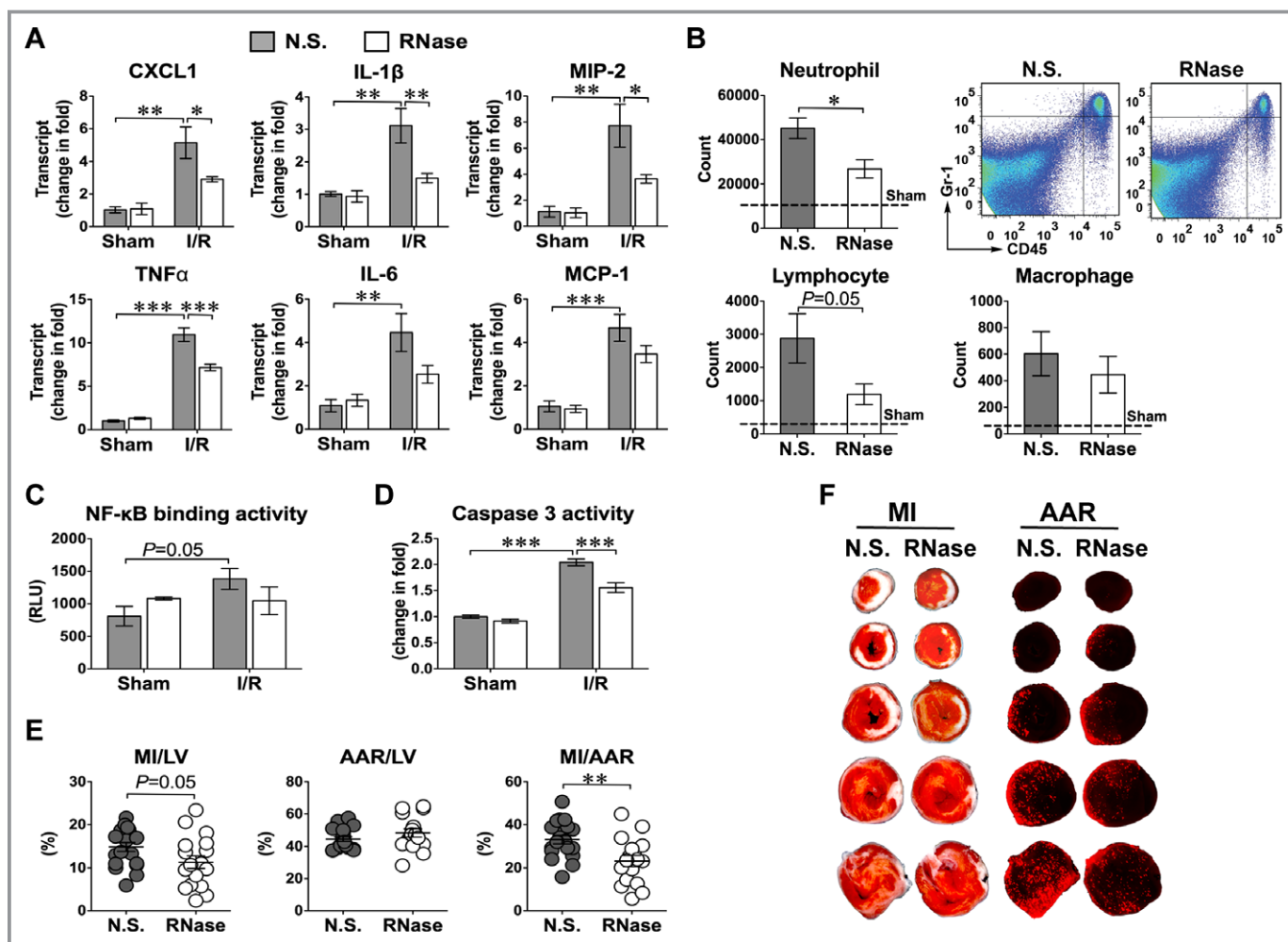


**Figure 10.** Effect of RNase administration on myocardial inflammation, apoptosis, and infarct sizes after I/R. **A**, Effect of RNase on myocardial cytokine mRNA. Mice were treated with N.S. or RNase and subjected to sham or I/R. Three hours after reperfusion, myocardial cytokines were analyzed by qRT-PCR. Sham,  $n=3$ ; I/R,  $n=5$ . **B**, Effect of RNase treatment on myocardial infiltration of CD45<sup>+</sup>Gr-1<sup>+</sup> neutrophil, CD3<sup>+</sup> T lymphocyte and F4/80<sup>+</sup> macrophage after I/R. A representative FACS plot of neutrophils is shown. **C**, Effect of RNase on myocardial NF- $\kappa$ B activity. IR. Sham,  $n=3$ ; I/R,  $n=5$ . **D**, Effect of RNase on myocardial caspase-3 activity after 4 hours of reperfusion. Sham,  $n=3$ ; I/R,  $n=5$ . **E**, Effect of RNase on MI after I/R.  $n=19$ /group. **F**, Representative of TTC staining (left) and fluorescent microsphere distribution (right) of myocardial sections from N.S.- or RNase-treated mice. AAR is indicated by the areas devoid of red fluorescent light and the infarct area shown as white. \* $P<0.05$ , \*\* $P<0.01$ , \*\*\* $P<0.001$ . AAR indicates area-at-risk; CXCL1, chemokine (C-X-C motif) ligand 1; I/R, ischemia/reperfusion; IFN, interferon; IL, interleukin; LV, left ventricular; MI, myocardial infarction; MCP-1, monocyte chemoattractant protein-1; MIP-2, macrophage inflammatory protein-2; NF- $\kappa$ B, nuclear factor-kappaB; N.S., normal saline; qRT-PCR, quantitative real time polymerase chain reaction; RLU, relative luminescence units; TNF, tumor necrosis factor; TTC, triphenyltetrazolium chloride.

that absence of TLR3-Trif signaling leads to reduced myocardial injury and improved LV function. It is noteworthy, however, that Trif<sup>-/-</sup> mice had much more dramatic reduction in MI size than TLR3<sup>-/-</sup> mice when compared with WT (68% versus 28% reduction in MI size). We speculate this might be due to the fact that Trif transduces the signaling from both TLR3 and TLR4. Deletion in Trif would result in blockage of TLR3 and a part of TLR4 signaling. In stark contrast to TLR2/4-MyD88 signaling, TLR3-Trif signaling appears to mediate I/R injury via a mechanism independent of inflammation since the absence of TLR3-Trif has no impact

on cardiac cytokine production or on neutrophil recruitment in response to I/R. Thus, these data suggest that despite its ability to mediate inflammatory cytokine response in immune cells and during viral myocarditis and bacterial sepsis,<sup>10,16–18</sup> TLR3-Trif signaling may make no major contribution to myocardial inflammation in response to I/R.

Type I IFN is the key downstream effector of TLR3-Trif signaling and plays a pivotal role in host antiviral defense.<sup>18</sup> Similar to viral myocarditis, I/R induces significant myocardial type I/II IFN response. However, absence of TLR3 or Trif did not affect the myocardial IFN response, suggesting that

I/R-induced IFN expression in the heart is probably not mediated by TLR3-Trif signaling. The fact that IFNAR<sup>-/-</sup> mice have the similar infarct size as WT mice demonstrates that type I IFN plays no major role in I/R-induced myocardial injury.

In the current study, we took 3 different approaches to detect myocardial apoptosis: ex vivo cardiac AV-750 FRI, DNA laddering, and caspase-3 activity. The fluorescent AV-750 construct has been used by our lab in a mouse model of I/R injury<sup>34</sup> and <sup>99</sup>Tc-labeled annexin-V used in patients to image myocardial injury.<sup>48</sup> We found that Trif deficiency led to significant attenuation of myocardial apoptosis after I/R injury. This is consistent with a previous in vitro study that demonstrates that Trif induces cellular apoptosis through a RIP/FADD/caspase-8-dependent pathway.<sup>49</sup> Thus, the current study establishes Trif signaling as a pathway in the heart that controls myocardial apoptosis and mediates myocardial injury during I/R.

To determine the role of exRNA in cardiomyocyte cytokine response and in ischemic myocardial injury, we first showed that under stressful conditions such as hypoxia/serum deprivation and myocardial I/R, cardiomyocytes and the heart, respectively, released substantial amount of RNA. Using a sensitive qRT-PCR, we detected the release of several miRNA (miR-208a, miR-499, miR-1, and miR-133) that are reportedly highly present in cardiomyocytes and in skeletal muscle cells with miR-208 expressed exclusively in the heart.<sup>50,51</sup> The significance of these miRNA in ischemic myocardial injury is evidenced by the fact that the circulating levels of these miRNA are dramatically elevated after acute MI compared with control subjects in patients as well as experimental models.<sup>52,53</sup> We also demonstrated that isolated cardiomyocytes responded to necrotic macrophages and cardiomyocytes and produced multiple cytokines such as IL-1 $\beta$ , MIP-2, IL-6, CXCL1, and MCP-1. The necrotic cell-induced cytokine response is dose-dependent and significantly attenuated by RNase treatment of the necrotic cells, but not by DNase. These data suggest that similar to what has been reported in a variety of cell types, RNA associated with damaged cells is capable of inducing cytokine responses in cardiomyocytes. Furthermore, we demonstrated that necrotic cell-induced MIP-2 production was significantly attenuated in TLR3<sup>-/-</sup> cardiomyocytes as compared with WT cells. This suggests that TLR3 mediates in part the necrotic cell-induced cytokine production in mouse cardiomyocytes.

In an effort to identify endogenous ligands for TLR3 that may mediate cardiac I/R injury, we explored the role of endogenous exRNA in cardiac I/R injury. We administered RNase before, during and after coronary occlusion. RNase has a small molecular weight (17 kDa) and a short plasma half-life (only min) with a rapid clearance primarily via kidney.<sup>54</sup> The protocol of RNase administration provided a markedly enhanced plasma RNase activity for up to at least 4 hours. However, it remains

unclear how complete the digestion of exRNA would be by the exogenously administered RNase in vivo as certain exosome-associated RNA could be protected from RNase digestion<sup>20</sup> and exRNA in the interstitial space might not be fully exposed to circulating RNase. Nevertheless, using the RNase delivering protocol, we demonstrated that mice treated with RNase had significantly reduced myocardial cytokine responses as well as caspase-3 activation following I/R. Most importantly, RNase administration also led to a significant reduction in MI size compared with normal saline treatment after I/R. Thus, we identify circulating exRNA as a significant contributor to myocardial inflammation and injury following coronary occlusion in the heart. These data are consistent with the theme that exRNA is increasingly recognized as an important player in diverse pathological conditions such as blood coagulation following carotid artery injury<sup>28</sup> and radiation-induced skin damage.<sup>14</sup> Of note, the fact that RNase administration and TLR3 deficiency confer similar cardiac protection against I/R injury (eg, reduced MI sizes and apoptosis) but differ in myocardial inflammation (eg, neutrophil infiltration and cytokine production) raises a possibility that exRNA and TLR3 may contribute to I/R injury via different signaling pathways. The possible role of TLR3 signaling in exRNA-mediated I/R injury remains to be investigated.

In summary, the current study indicates that circulating exRNA and TLR3-Trif signaling contribute to ischemic myocardial injury. RNase treatment or loss of TLR3-Trif signaling leads to reduced MI in a mouse model of I/R injury. Our data suggest that TLR3-Trif signaling contributes to ischemic myocardial injury most likely by mediating cardiac apoptosis and plays no major role in myocardial inflammation during I/R. Moreover, we propose that under ischemic condition, cardiomyocytes in vitro and cardiac tissue in vivo release RNA. Extracellular RNA in turn facilitates pro-inflammatory cytokine responses in cardiomyocytes and contributes to subsequent myocardial injury in the ischemic heart. Future studies will be needed to delineate the signaling mechanisms by which exRNA contributes to myocardial inflammation and injury during I/R.

## Sources of Funding

This work was supported in part by the National Institutes of Health grants R01GM-080906 and R01GM-097259 (to Dr Chao) and a mentored research award from International Anesthesia Research Society (to Dr Zou). Dr Chen was supported by a scholarship from Chinese Scholar Council.

## Disclosures

None.

## References

- Hoyert DL, Xu J. Deaths: preliminary data for 2011. *Natl Vital Stat Rep*. 2012;61:1–52.
- Yellon DM, Hausenloy DJ. Myocardial reperfusion injury. *N Engl J Med*. 2007;357:1121–1135.
- Eefting F, Rensing B, Wigman J, Pannekoek WJ, Liu WM, Cramer MJ, Lips DJ, Doevendans PA. Role of apoptosis in reperfusion injury. *Cardiovasc Res*. 2004;61:414–426.
- Akira S, Uematsu S, Takeuchi O. Pathogen recognition and innate immunity. *Cell*. 2006;124:783–801.
- Mann DL. The emerging role of innate immunity in the heart and vascular system: for whom the cell tolls. *Circ Res*. 2011;108:1133–1145.
- Chao W. Toll-like receptor signaling: a critical modulator of cell survival and ischemic injury in the heart. *Am J Physiol Heart Circ Physiol*. 2009;296:H1–H12.
- Ohashi K, Burkart V, Flohe S, Kolb H. Cutting edge: heat shock protein 60 is a putative endogenous ligand of the toll-like receptor-4 complex. *J Immunol*. 2000;164:558–561.
- Park JS, Svetkauskaite D, He Q, Kim JY, Strassheim D, Ishizaka A, Abraham E. Involvement of toll-like receptors 2 and 4 in cellular activation by high mobility group box 1 protein. *J Biol Chem*. 2004;279:7370–7377.
- Kariko K, Ni H, Capodici J, Lamphier M, Weissman D. mRNA is an endogenous ligand for toll-like receptor 3. *J Biol Chem*. 2004;279:12542–12550.
- Cavassani KA, Ishii M, Wen H, Schaller MA, Lincoln PM, Lukacs NW, Hogaboam CM, Kunkel SL. TLR3 is an endogenous sensor of tissue necrosis during acute inflammatory events. *J Exp Med*. 2008;205:2609–2621.
- Alexopoulou L, Holt AC, Medzhitov R, Flavell RA. Recognition of double-stranded RNA and activation of NF-kappaB by toll-like receptor 3. *Nature*. 2001;413:732–738.
- Guidotti LG, Chisari FV. Noncytolytic control of viral infections by the innate and adaptive immune response. *Annu Rev Immunol*. 2001;19:65–91.
- Brentano F, Schorr O, Gay RE, Gay S, Kyburz D. RNA released from necrotic synovial fluid cells activates rheumatoid arthritis synovial fibroblasts via toll-like receptor 3. *Arthritis Rheum*. 2005;52:2656–2665.
- Bernard JJ, Cowing-Zitron C, Nakatsuji T, Muehleisen B, Muto J, Borkowski AW, Martinez L, Greidinger EL, Yu BD, Gallo RL. Ultraviolet radiation damages self noncoding RNA and is detected by TLR3. *Nat Med*. 2012;18:1286–1291.
- Rasschaert J, Ladriere L, Urbain M, Dogusan Z, Katabua B, Sato S, Akira S, Gysemans C, Mathieu C, Eizirik DL. Toll-like receptor 3 and STAT-1 contribute to double-stranded RNA+ interferon-gamma-induced apoptosis in primary pancreatic beta-cells. *J Biol Chem*. 2005;280:33984–33991.
- Hardarson HS, Baker JS, Yang Z, Purevjav E, Huang CH, Alexopoulou L, Li N, Flavell RA, Bowles NE, Vallejo JG. Toll-like receptor 3 is an essential component of the innate stress response in virus-induced cardiac injury. *Am J Physiol Heart Circ Physiol*. 2007;292:H251–H258.
- Negishi H, Osawa T, Ogami K, Ouyang X, Sakaguchi S, Koshiba R, Yanai H, Seko Y, Shitara H, Bishop K, Yonekawa H, Tamura T, Kaisho T, Taya C, Taniguchi T, Honda K. A critical link between toll-like receptor 3 and type II interferon signaling pathways in antiviral innate immunity. *Proc Natl Acad Sci USA*. 2008;105:20446–20451.
- Riad A, Westermann D, Zietsch C, Savvatis K, Becher PM, Bereswill S, Heimesaat MM, Lettau O, Lassner D, Dorner A, Poller W, Busch M, Felix SB, Schultheiss HP, Tschope C. Trif is a critical survival factor in viral cardiomyopathy. *J Immunol*. 2011;186:2561–2570.
- Dinger ME, Mercer TR, Mattick JS. RNAs as extracellular signaling molecules. *J Mol Endocrinol*. 2008;40:151–159.
- Creemers EE, Tijssen AJ, Pinto YM. Circulating microRNAs: novel biomarkers and extracellular communicators in cardiovascular disease? *Circ Res*. 2012;110:483–495.
- Tijssen AJ, Pinto YM, Creemers EE. Circulating microRNAs as diagnostic biomarkers for cardiovascular diseases. *Am J Physiol Heart Circ Physiol*. 2012;303:H1085–H1095.
- Quinn SR, O'Neill LA. A trio of microRNAs that control toll-like receptor signalling. *Int Immunol*. 2011;23:421–425.
- Roy S, Sen CK. miRNA in innate immune responses: novel players in wound inflammation. *Physiol Genomics*. 2011;43:557–565.
- Roy S, Sen CK. miRNA in wound inflammation and angiogenesis. *Microcirculation*. 2012;19:224–232.
- Fabbri M, Paoone A, Calore F, Galli R, Gaudio E, Santhanam R, Lovat F, Fadda P, Mao C, Nuovo GJ, Zanesi N, Crawford M, Ozer GH, Wernicke D, Alder H, Caligiuri MA, Nana-Sinkam P, Perrotti D, Croce CM. microRNAs bind to toll-like receptors to induce prometastatic inflammatory response. *Proc Natl Acad Sci USA*. 2012;109:E2110–E2116.
- Roy S, Khanna S, Hussain SR, Biswas S, Azad A, Rink C, Gnyawali S, Shilo S, Nuovo GJ, Sen CK. MicroRNA expression in response to murine myocardial infarction: mir-21 regulates fibroblast metalloprotease-2 via phosphatase and tensin homologue. *Cardiovasc Res*. 2009;82:21–29.
- Lim DM, Wang ML. Toll-like receptor 3 signaling enables human esophageal epithelial cells to sense endogenous danger signals released by necrotic cells. *Am J Physiol Gastrointest Liver Physiol*. 2011;301:G91–G99.
- Kannemeier C, Shibamiya A, Nakazawa F, Trusheim H, Ruppert C, Markart P, Song Y, Tzima E, Kennerknecht E, Niepmann M, von Bruehl ML, Sedding D, Massberg S, Gunther A, Engelmann B, Preissner KT. Extracellular RNA constitutes a natural procoagulant cofactor in blood coagulation. *Proc Natl Acad Sci USA*. 2007;104:6388–6393.
- Yamamoto M, Sato S, Hemmi H, Hoshino K, Kaisho T, Sanjo H, Takeuchi O, Sugiyama M, Okabe M, Takeda K, Akira S. Role of adaptor Trif in the myd88-independent toll-like receptor signaling pathway. *Science*. 2003;301:640–643.
- Feng Y, Zhao H, Xu X, Buys ES, Raheer MJ, Bopassa JC, Thibault H, Scherrer-Crosbie M, Schmidt U, Chao W. Innate immune adaptor myd88 mediates neutrophil recruitment and myocardial injury after ischemia-reperfusion in mice. *Am J Physiol Heart Circ Physiol*. 2008;295:H1311–H1318.
- Zou L, Feng Y, Chen YJ, Si R, Shen S, Zhou Q, Ichinose F, Scherrer-Crosbie M, Chao W. Toll-like receptor 2 plays a critical role in cardiac dysfunction during polymicrobial sepsis. *Crit Care Med*. 2010;38:1335–1342.
- Feng Y, Zou L, Si R, Nagasaka Y, Chao W. Bone marrow myd88 signaling modulates neutrophil function and ischemic myocardial injury. *Am J Physiol Cell Physiol*. 2010;299:C760–C769.
- Zou L, Feng Y, Zhang M, Li Y, Chao W. Nonhematopoietic toll-like receptor 2 contributes to neutrophil and cardiac function impairment during polymicrobial sepsis. *Shock*. 2011;36:370–380.
- Li Y, Si R, Feng Y, Chen HH, Zou L, Wang E, Zhang M, Warren HS, Sosnovik DE, Chao W. Myocardial ischemia activates an injurious innate immune signaling via cardiac heat shock protein 60 and toll-like receptor 4. *J Biol Chem*. 2011;286:31308–31319.
- Chao W, Shen Y, Zhu X, Zhao H, Novikov M, Schmidt U, Rosenzweig A. Lipopolysaccharide improves cardiomyocyte survival and function after serum deprivation. *J Biol Chem*. 2005;280:21997–22005.
- Zhu X, Zhao H, Graveline AR, Buys ES, Schmidt U, Bloch KD, Rosenzweig A, Chao W. Myd88 and NOS2 are essential for toll-like receptor 4-mediated survival effect in cardiomyocytes. *Am J Physiol Heart Circ Physiol*. 2006;291:H1900–H1909.
- Akira S. Toll-like receptor signaling. *J Biol Chem*. 2003;278:38105–38108.
- Kaiser WJ, Offermann MK. Apoptosis induced by the toll-like receptor adaptor Trif is dependent on its receptor interacting protein homotypic interaction motif. *J Immunol*. 2005;174:4942–4952.
- Ruckdeschel K, Pfaffinger G, Haase R, Sing A, Weighardt H, Hacker G, Holzmann B, Heesemann J. Signaling of apoptosis through TLRs critically involves toll/IL-1 receptor domain-containing adapter inducing IFN-beta, but not Myd88, in bacteria-infected murine macrophages. *J Immunol*. 2004;173:3320–3328.
- De Trez C, Pajak B, Brait M, Glaichenhaus N, Urbain J, Moser M, Lauvau G, Muraille E. TLR4 and toll-IL-1 receptor domain-containing adapter-inducing IFN-beta, but not myd88, regulate *Escherichia coli*-induced dendritic cell maturation and apoptosis in vivo. *J Immunol*. 2005;175:839–846.
- Colamonici OR, Domanski P. Identification of a novel subunit of the type I interferon receptor localized to human chromosome 21. *J Biol Chem*. 1993;268:10895–10899.
- Muller U, Steinhoff U, Reis LF, Hemmi S, Pavlovic J, Zinkernagel RM, Aguet M. Functional role of type I and type II interferons in antiviral defense. *Science*. 1994;264:1918–1921.
- Li Q, Kim Y, Namm J, Kulkarni A, Rosania GR, Ahn YH, Chang YT. RNA-selective, live cell imaging probes for studying nuclear structure and function. *Chem Biol*. 2006;13:615–623.
- Arslan F, Smeets MB, O'Neill LA, Keogh B, McGuirk P, Timmers L, Tersteeg C, Hoefer IE, Doevendans PA, Pasterkamp G, de Kleijn DP. Myocardial ischemia/reperfusion injury is mediated by leukocytic toll-like receptor-2 and reduced by systemic administration of a novel anti-toll-like receptor-2 antibody. *Circulation*. 2010;121:80–90.
- Oyama J, Blais C Jr, Liu X, Pu M, Kobzik L, Kelly RA, Bourcier T. Reduced myocardial ischemia-reperfusion injury in toll-like receptor 4-deficient mice. *Circulation*. 2004;109:784–789.
- Shimamoto A, Chong AJ, Yada M, Shomura S, Takayama H, Fleisig AJ, Agnew ML, Hampton CR, Rothnie CL, Spring DJ, Pohlman TH, Shimpo H, Verrier ED. Inhibition of toll-like receptor 4 with eritoran attenuates myocardial ischemia-reperfusion injury. *Circulation*. 2006;114:I270–I274.



47. Schmid-Schonbein GW. Toll-like receptor signaling mechanisms in hostile neutrophils. Focus on "bone marrow myd88 signaling modulates neutrophil function and ischemic myocardial injury." *Am J Physiol Cell Physiol.* 2010;299:C731–C732.
48. Hofstra L, Liem IH, Dumont EA, Boersma HH, van Heerde WL, Doevendans PA, De Muinck E, Wellens HJ, Kemerink GJ, Reutelingsperger CP, Heidendal GA. Visualisation of cell death in vivo in patients with acute myocardial infarction. *Lancet.* 2000;356:209–212.
49. Han KJ, Su X, Xu LG, Bin LH, Zhang J, Shu HB. Mechanisms of the Trif-induced interferon-stimulated response element and NF-kappaB activation and apoptosis pathways. *J Biol Chem.* 2004;279:15652–15661.
50. Fichtlscherer S, Zeiher AM, Dimmeler S. Circulating microRNAs: biomarkers or mediators of cardiovascular diseases? *Arterioscler Thromb Vasc Biol.* 2011;31:2383–2390.
51. van Rooij E, Sutherland LB, Qi X, Richardson JA, Hill J, Olson EN. Control of stress-dependent cardiac growth and gene expression by a microRNA. *Science.* 2007;316:575–579.
52. D'Alessandra Y, Devanna P, Limana F, Straino S, Di Carlo A, Brambilla PG, Rubino M, Carena MC, Spazzafumo L, De Simone M, Micheli B, Biglioli P, Achilli F, Martelli F, Maggolini S, Marenzi G, Pompilio G, Capogrossi MC. Circulating microRNAs are new and sensitive biomarkers of myocardial infarction. *Eur Heart J.* 2010;31:2765–2773.
53. Wang GK, Zhu JQ, Zhang JT, Li Q, Li Y, He J, Qin YW, Jing Q. Circulating microRNA: a novel potential biomarker for early diagnosis of acute myocardial infarction in humans. *Eur Heart J.* 2010;31:659–666.
54. Baynes JW, Wold F. Effect of glycosylation on the in vivo circulating half-life of ribonuclease. *J Biol Chem.* 1976;251:6016–6024.